Journal of Experimental & Theoretical Artificial Intelligence
Vol. 00, No. 00, Month 2013, 1–20

RESEARCH ARTICLE

Relative Observation for Multi-robot Collaborative Localization Based on Multi-source Signals

Qirong Tang and Peter Eberhard*

Institute of Engineering and Computational Mechanics, University of Stuttgart
Pfaffenwaldring 9, 70569 Stuttgart, Germany
(*Received 00 Month 2013; final version received 00 Month 2013*)

This paper describes a synthesizing method for multi-robot collaborative localization. A distributed extended Kalman filter based on robot odometry and external North Star signals for data fusion is first designed for the localization of individuals in the robot group. Relying on relative observation by infrared sensors and gyroscopes mounted on robots, and the 'uncertainty volume' strategy, the positions estimated by extended Kalman filters are further corrected for precising the localization process. The localization accuracy based on different sensing regimes is tested. Sensor correlations and uncertainties are analyzed for predicting error propagation and to accommodate sensing deviations. The multi-source signals are then synthesized for the collaborative localization for a multi-robot system without introducing excessive computation. Finally, this work is verified by both simulation and experiments with real robots, i.e. the Festo Robotinos under different scenarios.

Keywords: multi-robot; relative observation; multi-source signals; collaborative localization; North Star; extended Kalman filter

1. Introduction

Localization has been recognized as one of the fundamental problems in mobile robotics since it frequently becomes the barrier for executing many of the tasks, e.g., exploration (Grabowski et al. 2000), surveillance (Dhariwal and Sukhatme 2007), and search (Tang 2012). Many solutions have been provided in related fields for solving this problem which include the commonly used sensor-based methods and also some soft computing solutions based on source signals originating from sensors. For examples, in recent years researchers pay efforts on methods of topology (Murillo, Guerrero, and Sagüés 2007; Ferdaus 2008; McLurkin 2009), probabilistic (Thrun, Burgard, and Fox 2005; Yang 2008), as well as fuzzy logic (Maaref and Barret 2002; Molhim citeyearMolhim2002; Cao 2009) for robot localization.

From the perspective of localization utilization, there are basically three kinds of localization usages for mobile robots. The first kind is using localization for a single robot, the second one focuses on the localization for multiple robots as a whole, whereas the third kind of localization orients for multi-robot systems where correlations between individuals for realizing collaborative localization exist. The last one is also the research objective of this investigation.

Collaborative localization, sometimes refereed to as cooperative localization, is an efficient means for estimating the joint state of all the robots via information sharing among the members of the group. In this case, each robot may be correlated by internal peers. Because of the collaboration and correlation, researchers

*Corresponding author. Email: peter.eberhard@itm.uni-stuttgart.de

usually need to use several kinds of sensors simultaneously. Each kind of sensor is in charge of one or more specific purpose. Afterwards, questions like sensor data fusion, correlation calculation, uncertainty analysis, and error estimation have to be considered. Therefore, dealing with data from multi-source signals, improving the localization accuracy by relative observation or information sharing, and reducing computational cost for relatively simple robots become the critical issues which are concerned by this study.

This paper is organized as follows. Section 2 analyzes the state-of-the-art of related researches for multi-robot localization while Section 3 introduces the investigated omnidirectional mobile robot. Section 4 elaborates the localization scheme for a single robot and extensions for a multi-robot system are described in Section 5. Simulation investigations are demonstrated in Section 6 where sensor noise is mimicked according to the used hardware. Experiments with real robots are performed in Section 7. Section 8 gives results and performs discussions on the obtained results. Conclusions are given in Section 9 to close this paper.

2. Related Researches for Multi-robot Localization

Multi-robot or swarm robotic systems can fulfill many tasks that a single robot can not. However, the localization issue which exists in the single robot application won't vanish automatically when considering the multi-robot case. On the one hand, the localization of a multi-robot system is even more challenging since the localized deviations may lead to collisions among the robots. On the other hand, multi-robot systems can perform collaboration between the individuals which may make it possible for a team of robots to get localized easier and more precise than a single robot.

The Monte Carlo method is one of the most popular approaches for robot localization. It provides a good tradeoff between accuracy and robustness. Some investigations use it for mobile robots localization, e.g., in (Özkucur, Kurt, and Akın 2009) the Monte Carlo localization for the single robot case is extended using negative landmark information and shared belief state in addition to perception for multi-robot localization, (Fox et al. 2000) modify Monte Carlo and Markov methods for multi-robot localization in which probabilistic algorithms are used to synchronize each robot's belief. Using particle filters for tracking a probability distribution of possible robot poses is the underlying principle when employing Monte Carlo based methods. One exemplary application of this principle can be found in (Marchetti, Grisetti, and Iocchi 2007). Another very classical application based on a probabilistic method is shown in (Thrun 1998), where the Bayes rule is employed to incorporate sensor data into internal beliefs of robots.

The investigation described in (Roumeliotis and Bekey 2002) contributes decentralized and distributed architectures for multi-robot localization. The research (Howard, Matark, and Sukhatme 2002) performs localization by relying on the probabilistic approach of maximum likelihood estimation. The work done in (Madhavan, Fregene, and Parker 2004) is oriented for an outdoor environment where the global positioning system (GPS) is applied. However, GPS doesn't effectively work within buildings, and even outdoors, GPS is vertically very challenged. Due to attenuation and scattering, GPS falls apart indoors. The work in (Caglioti, Citterio, and Fossati 2006) uses a minimum entropy approach to minimize sensor uncertainty. As a result, these studies for multi-robot localization greatly increase the computational burden and also involve more interferences.

(Gasparri, Panzieri, and Pascucci 2009) provide a spatially structured genetic algorithm for multi-robot localization, however, the relative pose among robots

are just assumed to be available. That investigation was verified by simulation only. Recently 'Encounter Averaging' was provided which averages the location estimations of two robots whenever they get close enough, details can be found in (Elor and Bruckstein 2012). (Wang et al. 2009) use relative bearing for multi-robot cooperative localization, however, some singularities are not well addressed.

Considerations in this study are to use as simple algorithms as possible for localization and the robots in the group should only be equipped with simple sensors and restricted memory. Our preferred manner to realize multi-robot collaborative localization is using relative observations, which are computationally light. Most researches in this area are focusing on differentially driven mobile robots, whereas, this study takes the omnidirectional mobile robot as its research objective.

3. Introduction of the Investigated Festo Robotino Robot

In recent years omnidirectional mobile robots attracted researchers interest due to their unique features, see examples in (Wu 2005) and (Liu et al. 2008). This study presents methods for the collaborative localization of one kind of omnidirectional mobile robots, the Festo Robotinos, which are used for our purpose of searching targets in environments.

A Robotino is an omnidirectional and holonomic mobile robot which is mainly developed by Festo Didactic in Germany. This creative product orients for both education and research and it won the Worlddidac award and the German reddot design award. For a better understanding, the Robotino and its main components are illustrated in Figure 1.

Figure 1. Festo Robotino and its main components (photo from (Bliesener et al. 2007))

There are three omni-wheel units installed on each Robotino which make possible for the robot to move in any direction whatever the current orientation is. However, this omnidirectional feature also brings difficulties for robot localization since it couples translational errors and rotational errors. Besides the originally equipped sensors like, e.g., infrared distance sensors and protective sensors, one can also extend the interfaces for peripheral devices like a gyroscope and a North Star (NS) positioning system which are used in this investigation.

4. Localization for a Single Robot Based on an Extended Kalman Filter

One must consider the localization ability of moving robots for successfully performing tasks like navigation or trajectory tracking. The functionality of localiza-

tion answers the question of 'Where am I?'. Combined with control techniques, it enables to drive robots to a desired position with acceptable accuracy. This study first builds strategies for the localization of each Robotino individually before the collaborative localization is done in a systematic manner.

The robot uses sensors to localize its current pose. However, the sensor data always contains noise which requires to improve sensor data before taking them as the localization outcome. The overall scheme for the localization and position control of a single Robotino is shown in Figure 2 in which a closed-loop feedback control is included. The robot's 'actual' position and orientation are measured not only by on-body encoders based odometry but also by an external North Star navigation system. The measured poses are then processed in an extended Kalman filter (EKF). With data fusion in EKF, it gives a filtered position and orientation which are compared to the desired set point. The resulting deviation $[\Delta x \ \ \Delta y \ \ \Delta\phi]_g$ drives the robot to approach the purposed pose. By using such a strategy this research first wants to improve the localization accuracy of a single robot. The used scheme is valid for all the robots in the group independently thus it is in a distributed EKFs fashion. Then it is extended for a multi-robot. In the following first an investigation on how to validate this strategy is performed.

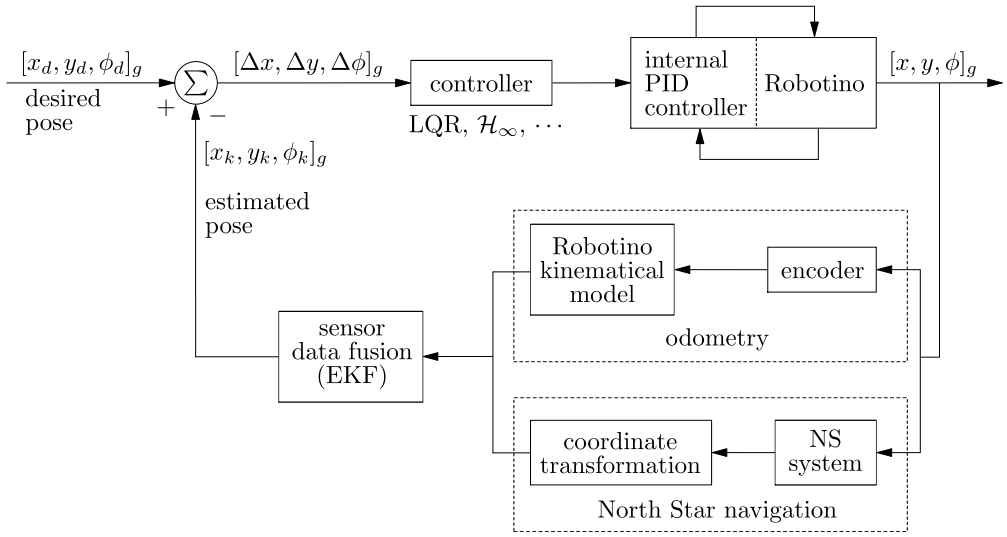

Figure 2. Scheme of localization and position control for a single Robotino

In this study we use robot odometry and a North Star positioning system to perform localization. However, neither of them provide enough accuracy. Robotino's odometry corresponds to the measurement of wheel rotation by using motor encoders to continually update incremental wheel information. The current robot pose is then determined by time integration adding to the previously known pose. However, odometry only yields good local performance. Errors can accumulate for long distances or under adverse conditions. The error sources can come, e.g., from wheel slippage, non symmetrical robot structure and non precise assembling. The NS system also involves noise. For example, the NS detector will exhibit nonlinear absolute localization responses and this nonlinearity will increase as the infrared projector's light spots move away from the center of the detectors view field. Besides this, position and orientation errors will also be produced when the detector is tilted from the plane of localization environment, typically, the floor. Thus, the questions are, e.g., how to use the pose information for robot position control, or how to weight the measurements from different sensors. From another side, we want to improve the position accuracy of robots while not putting too much burden on

the robot hardware. Due to these reasons, using methods to perform sensor data fusion will be a good choice based on the information from odometry and the NS system.

The Kalman filter (Kalman 1960) fits well to our requirement. A Kalman filter is an estimator for estimating the instantaneous 'state' of a linear dynamic system perturbed by white noise (Grewal and Andrews 2008). In our case, it can fuse the information from odometry and NS meanwhile reduce noise affection.

The estimated object in this study is a nonlinear process thus it is required to use the extended Kalman filter (Grewal and Andrews 2008). Procedures of an EKF in general are composed by five steps. First, performing the a-priori estimation of the state $\boldsymbol{x}$ (robot pose) by

$$\boldsymbol{x}(k)^{-} = \boldsymbol{f}(\hat{\boldsymbol{x}}(k-1), \boldsymbol{u}(k-1), \boldsymbol{0}). \tag{1}$$

Here k is the process step. We use the super script 'minus' to indicate the a-priori status. In (1), $\boldsymbol{f}$ is a nonlinear function which relates the state at step $k-1$ to step k, $\boldsymbol{u}$ is the optional control input.

According to the Robotino model, the discrete a-priori pose estimation in this application is given by

$$\begin{bmatrix} x_g(k)^{-} \\ y_g(k)^{-} \\ \phi_g(k)^{-} \end{bmatrix} = \begin{bmatrix} \hat{x}_g(k-1) \\ \hat{y}_g(k-1) \\ \hat{\phi}_g(k-1) \end{bmatrix} + \Delta t \begin{bmatrix} \cos(\hat{\phi}_g(k-1)) & -\sin(\hat{\phi}_g(k-1)) & 0 \\ \sin(\hat{\phi}_g(k-1)) & \cos(\hat{\phi}_g(k-1)) & 0 \\ 0 & 0 & 1 \end{bmatrix} \cdot \begin{bmatrix} \dot{x}_l(k-1) \\ \dot{y}_l(k-1) \\ \dot{\phi}_l(k-1) \end{bmatrix} \tag{2}$$

in which one writes the wheels angular velocities together with wheel radii and geometric structure, see Figure 3, of the Robotino to get the velocities $\dot{x}_l(k-1), \dot{y}_l(k-1)$ and $\dot{\phi}_l(k-1)$. They are the last step's velocities given in the robot body frame, a detailed similar derivation can be found in (Tang 2012; Eberhard and Tang 2013) in which these velocities are further corrected due to odometry correction. However, in this investigation they remain in the original form since we focus on the accuracy improvement by EKF and relative observation between robots. For the extended Kalman filter to perform recursions for robot pose estimation one needs to know the function $\boldsymbol{f}$ explicitly. Based on (2), one can write its three dimensions separately which yields

$$\begin{aligned} f_x = x_g(k)^{-} =& \hat{x}_g(k-1) + \Delta t \cos(\hat{\phi}_g(k-1))\, \dot{x}_l(k-1) \\ & - \Delta t \sin(\hat{\phi}_g(k-1))\, \dot{y}_l(k-1) + \underbrace{0}_{\cdot\, \Delta t\, \dot{\phi}_l(k-1)}, \end{aligned} \tag{3}$$

$$\begin{aligned} f_y = y_g(k)^{-} =& \hat{y}_g(k-1) + \Delta t \sin(\hat{\phi}_g(k-1))\, \dot{x}_l(k-1) \\ & + \Delta t \cos(\hat{\phi}_g(k-1))\, \dot{y}_l(k-1) + \underbrace{0}_{\cdot\, \Delta t\, \dot{\phi}_l(k-1)}, \end{aligned} \tag{4}$$

$$f_\phi = \phi_g(k)^{-} = \hat{\phi}_g(k-1) + \underbrace{0}_{\cdot\, \Delta t\, \dot{x}_l(k-1)} + \underbrace{0}_{\cdot\, \Delta t\, \dot{y}_l(k-1)} + \Delta t\, \dot{\phi}_l(k-1). \tag{5}$$

Next, one needs to calculate the a-priori estimate of the error covariance

$$\boldsymbol{P}(k)^{-} = \bar{\boldsymbol{A}}(k) \cdot \boldsymbol{P}(k-1) \cdot \bar{\boldsymbol{A}}^{T}(k) + \boldsymbol{W}(k) \cdot \boldsymbol{Q}(k-1) \cdot \boldsymbol{W}^{T}(k). \tag{6}$$

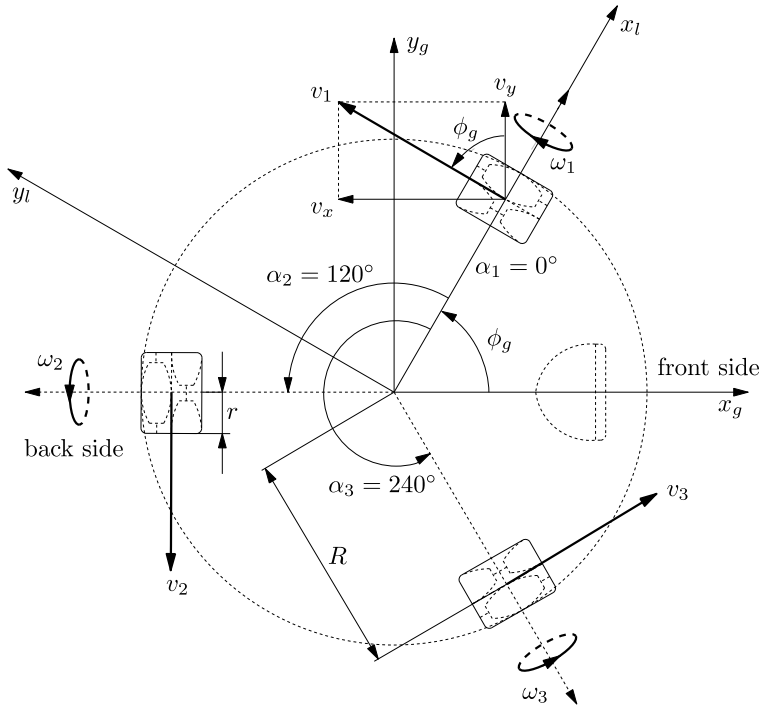

Figure 3. Geometry diagram and kinematic relations of Robotino base

Here, $\boldsymbol{Q}(k-1)$ is the process noise covariance and $\bar{\boldsymbol{A}}(k)$ as well as $\boldsymbol{W}(k)$ are matrices containing partial derivatives

$$\bar{A}_{i,j}(k) = \frac{\partial f_i}{\partial x_j}(\hat{\boldsymbol{x}}(k-1), \boldsymbol{u}(k-1), \boldsymbol{0}), \tag{7}$$

$$W_{i,j}(k) = \frac{\partial f_i}{\partial w_j}(\hat{\boldsymbol{x}}(k-1), \boldsymbol{u}(k-1), \boldsymbol{0}). \tag{8}$$

The matrix $\boldsymbol{W}(k)$ depends on the process noise. Thus, for obtaining $\boldsymbol{P}$ one first needs to calculate the matrices $\bar{\boldsymbol{A}}(k)$ and $\boldsymbol{W}(k)$ according to (7) and (8) combined with the process functions (3)-(5). In this application it yields

$$\begin{aligned}\bar{\boldsymbol{A}}(k) &= \left(\bar{A}_{i,j}(k)\right)_{3\times 3} \\ &= \begin{bmatrix} 1 & 0 & -\Delta t\, \sin(\hat{\phi}_g(k-1))\, \dot{x}_l(k-1) - \Delta t\, \cos(\hat{\phi}_g(k-1))\, \dot{y}_l(k-1) \\ 0 & 1 & \Delta t\, \cos(\hat{\phi}_g(k-1))\, \dot{x}_l(k-1) - \Delta t\, \sin(\hat{\phi}_g(k-1))\, \dot{y}_l(k-1) \\ 0 & 0 & 1 \end{bmatrix},\end{aligned} \tag{9}$$

$$\boldsymbol{W}(k) = (W_{i,j}(k))_{3\times 3} = \begin{bmatrix} \Delta t\, \cos(\hat{\phi}_g(k-1)) & -\Delta t\, \sin(\hat{\phi}_g(k-1)) & 0 \\ \Delta t\, \sin(\hat{\phi}_g(k-1)) & \Delta t\, \cos(\hat{\phi}_g(k-1)) & 0 \\ 0 & 0 & \Delta t \end{bmatrix}. \tag{10}$$

Due to the definition in (8), $\boldsymbol{W}$ contains entries which are the partial derivatives of $\boldsymbol{f}$ with respect to $\boldsymbol{w}$. However, practically $\boldsymbol{w}$ is always calculated through the

variables of noise sources. In this application the considered noises are contained in robot's body velocities which originally come from robot motors. Thus, here the entries of matrix $\boldsymbol{W}$ become the partial derivatives of $\boldsymbol{f}$ with respect to $\dot{x}_l(k-1), \dot{y}_l(k-1)$ and $\dot{\phi}_l(k-1)$.

After this the extended Kalman filter gets into the processes of correction. Thus, the Kalman gain matrix must be calculated which is

$$\boldsymbol{K}(k) = \boldsymbol{P}(k)^- \cdot \bar{\boldsymbol{H}}^T(k) \cdot (\bar{\boldsymbol{H}}(k) \cdot \boldsymbol{P}(k)^- \cdot \bar{\boldsymbol{H}}^T(k) + \boldsymbol{V}(k) \cdot \boldsymbol{R}(k) \cdot \boldsymbol{V}^T(k))^{-1}. \quad (11)$$

In this investigation it is degenerated to

$$\boldsymbol{K}(k) = \boldsymbol{P}(k)^- \cdot (\boldsymbol{P}(k)^- + \boldsymbol{R}(k))^{-1} \quad (12)$$

since both $\bar{\boldsymbol{H}}(k)$ and $\boldsymbol{V}(k)$ are unit matrices here. Matrix $\bar{\boldsymbol{H}}(k)$ is due to the external NS device while $\boldsymbol{V}(k)$ depends on the measurement noise of the NS. The matrices $\boldsymbol{Q}$ in (6) and $\boldsymbol{R}$ in (12) are the process noise covariance and measurement noise covariance, respectively, and both of them might change during recursion. Both $\boldsymbol{Q}$ and $\boldsymbol{R}$ are updated based on the newly measurements in each step and they become two of the uncertainty sources. A workable formation of $\boldsymbol{Q}$ and $\boldsymbol{R}$ can take reference from the work (Eberhard and Tang 2013). In our case, $\boldsymbol{Q}$ essentially depends on the noise of reading the motor speeds and $\boldsymbol{R}$ depends on the measurement noise from North Star.

Then, the a-posteriori pose correction is performed in general by

$$\hat{\boldsymbol{x}}(k) = \boldsymbol{x}(k)^- + \boldsymbol{K}(k) \cdot (\boldsymbol{z}(k) - \boldsymbol{h}(\boldsymbol{x}(k)^-, \boldsymbol{0})). \quad (13)$$

Correspondingly in this investigation it is governed by

$$\begin{bmatrix} \hat{x}_g(k) \\ \hat{y}_g(k) \\ \hat{\phi}_g(k) \end{bmatrix} = \begin{bmatrix} x_g(k)^- \\ y_g(k)^- \\ \phi_g(k)^- \end{bmatrix} + \boldsymbol{K}(k) \cdot \left(\begin{bmatrix} z_x(k) \\ z_y(k) \\ z_\phi(k) \end{bmatrix} - \begin{bmatrix} x_g(k)^- \\ y_g(k)^- \\ \phi_g(k)^- \end{bmatrix} \right). \quad (14)$$

We use the super script 'hat' to indicate the a-posteriori status. In (13) $\boldsymbol{h}$ is the measurement function. In each recursion loop, the result from (14) is feed back to the desired pose for position control. The variables z_x, z_y and z_ϕ in (14) are the three dimensions of the pose measured by the external North Star system. The NS system is an infrared (IR) light based positioning device. It is mainly composed by two parts, one projector, see Figure 4, and one detector, see Figure 5. The NS system enables position and heading awareness in mobile robots. When the projector emits IR light which is reflected by the ceiling, the IR detector which is mounted on the Robotino can receive the light signals and takes such signals as uniquely identifiable landmarks. By this, the robot can determine its relative position and direction. After calibration and coordination, it provides indoor global pose information to the robot. The NS system breaks the 'line-of-sight' barrier of previous light beacon systems with simplicity and reliability since its IR light is reflected by the ceiling. This North Star positioning system can be used for several robots simultaneously by using different channels identified by varied frequency ranges. This reduces the coordination errors compared to the situation where each robot has its own global frame. Therefore, it also improves the positioning accuracy.

Since only a rough robot pose can be obtained when using only odometry, it can be advantageous to add this external NS device which can give additional informa-

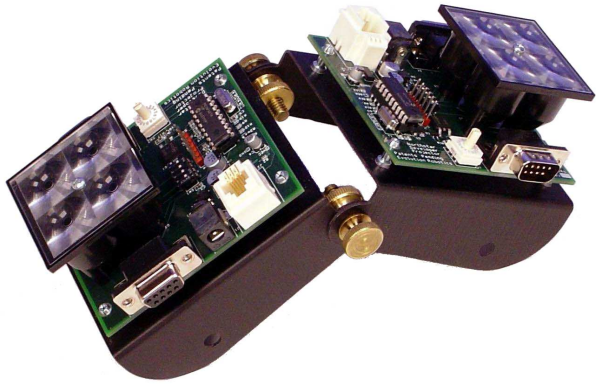

Figure 4. North Star projector (two emitter clusters)

Figure 5. North Star detector

tion independent on odometry. This standalone data is used for pose estimation through data fusion within an extended Kalman filter.

Afterwards, the prediction covariance is updated for the next round of recursion which is governed by

$$\boldsymbol{P}(k) = (\boldsymbol{I} - \boldsymbol{K}(k) \cdot \bar{\boldsymbol{H}}(k)) \cdot \boldsymbol{P}(k)^{-}. \tag{15}$$

Here, it is simplified to

$$\boldsymbol{P}(k) = (\boldsymbol{I} - \boldsymbol{K}(k)) \cdot \boldsymbol{P}(k)^{-}. \tag{16}$$

In both (15) and (16) $\boldsymbol{I}$ is a 3×3 unit matrix. Equations (1)-(16) contain all the EKF procedures and they are performed in a loop to promote the process of the system. From a mathematical point of view, in (14) $\boldsymbol{K}(k)$ is just a scaling factor to the two items, $\boldsymbol{x}(k)^{-}$ and $\boldsymbol{z}(k)$. However, physically the Kalman gain weights two sensor measurements, the odometry and North Star, by considering both of the sensors noises and uncertainties. Through this method, the information from both odometry and North Star are fused.

5. Extensions for Multi-robot Collaborative Localization

The method for robot localization shown in this study is performed in a distributed fashion, i.e., each robot in the group can be localized by an individual EKF applied on its own. Therefore, further improving the localization quality by benefiting from other robots in the group becomes an interesting and important topic.

5.1 *Theoretical Support*

The potential localization improvement of a robot under a distributed EKF is obvious. Each robot in this instance relies on its own resources rather than combining information from other agents in the group. Integrating measured information taken from different robots can obtain better performance. This is so called 'cooperative localization' or 'collaborative localization', i.e., let the current robot benefit from information collected by others. However, multi-robot collaborative localization introduces a new challenge since it needs to gather information from other entities. Thus, issues like uncertainty representation, relative observation, data association and so on have to be addressed.

For the uncertainty representation, we utilize the benefits from EKFs directly. Since the distributed EKF involves one task of calculating prediction error covariance, we take this prediction covariance, see Equation (16), as the uncertainty. This is a reuse of the previously obtained data which saves considerable computational cost. Therefore, robot i at the current step keeps an uncertainty representation of $\boldsymbol{P}_i(k)$. Unfortunately, this expression is not convenient for comparison since it is a matrix. This study provides the idea of an 'uncertainty volume' to evaluate the noise and uncertainty. One knows that in an Euclidean space, the determinant of a square matrix describes a super volume. So, we use $\det(\boldsymbol{P}_i)$ to evaluate the extent of uncertainty.

The challenge of relative observation actually implicates three aspects which are detection, judgment and making decision. Omnidirectional Robotinos are equipped with a ring of infrared sensors. They are capable of detecting nearby obstacles and also other robots. The characteristic of this infrared sensor is shown in Figure 6.

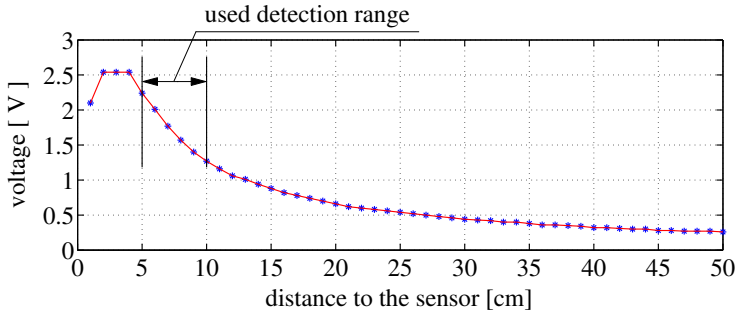

Figure 6. The characteristics curve of the infrared distance sensor

For accuracy purpose we only use the sensitive and linearizable detection range of the sensor which is [5 cm, 10 cm]. That is to say, we only read the detection data which corresponds to the distance of 5 cm to 10 cm away from the sensor in our relative observation scenario, see in Figure 6 the marked range. This is so because from experiments we noticed that the detection certainty within this range is better than EKF localization. Hence, we believe the localization accuracy can be improved by relative observation under this condition. So, robot i gives judgment and takes only robots which locate 5 cm to 10 cm away from him as its relevant neighbors. The relative observation only happens between these relevant neighbors. Infrared sensors are in this case responsible for obtaining relative position, i.e., the x and y directions relative distances. Relative orientation is performed via the subtraction of absolute orientation angles of two robots relying on digital gyroscopes.

The most important process of multi-robot collaborative localization comes from data association. One must find suitable strategies to deal with the data. Many researches just simply skip this part or assume there exist such strategies and verify only in simulation (Gasparri, Panzieri, and Pascucci 2009; Wang et al. 2009). Some other previous studies conducted complicated data association methods (Lee et al. 2008; Franklin et al. 2010), however, they are difficult for practical implementations. In contrast to the methods used in other studies, the strategy taken in this investigation is natural and easy to be implemented. Whenever a robot perceives a relevant neighbor, first of all their relevance is judged according to their distance. If they are relevant, their prediction covariances is compared. The one that has a higher estimation uncertainty should learn from the robot who has a better estimation belief, i.e., has lower uncertainty. One uses $\hat{\boldsymbol{p}}_{i,\,\mathrm{EKF}}$ and $\hat{\boldsymbol{p}}_{j,\,\mathrm{EKF}}$ to indicate the EKF estimated poses for robot i and robot j, respectively. Similarly, their prediction covariances are described by $\boldsymbol{P}_{i,\,\mathrm{EKF}}$ and $\boldsymbol{P}_{j,\,\mathrm{EKF}}$. Relative pose is

expressed by $\boldsymbol{p}_{\text{rel}}$. Thus, if the pose of robot i has lower belief compare to robot j, its learning process is governed by

$$\hat{\hat{\boldsymbol{p}}}_i = \hat{\boldsymbol{p}}_{j,\,\text{EKF}} + \boldsymbol{p}_{\text{rel}} \tag{17}$$

in which $\boldsymbol{p}_{\text{rel}}$ contains relative position from infrared distance sensors and relative orientation obtained by gyroscopes. Observations from these sensors are then organically integrated with the EKF estimation to update a belief state for the positions and orientations of all the robots.

We know from the hardware characteristics that the measurement errors of infrared sensors and gyroscopes within the relevant range are smaller than the prediction error from EKF which means (17) will result in a prediction covariance with the values between those of relative observation and those from EKF. However, the measurements from relative observation are independent to the measurements involved in EKF. One has to calculate the prediction covariance from relative observation originating from infrared sensors and gyroscopes if adhering to use this information. In addition, a scheme to associate the estimation covariances both from EKF and relative observation is demanded, which unfortunately increases the computational cost. Therefore, in this investigation we directly take its own EKF prediction covariance as the current new covariance for pose estimation. Actually, this is a conservative usage and the practical situation is better. Equation (17) in this case improves the pose estimation for robot i, what's more, it also positively affects the robots who haven't joined this pair of relative observation since the corrected robot i will provides information to them during the next round of updates.

We choose a random sequence for relative observation in the case that one robot is relevant to several of its neighbors. During one round of relative observation, it also requires that each robot maximally once performs effective relative observation and correspondingly only one time of further correction is taken to the robot pose after the EKF estimation.

5.2 *Implementation Steps*

The procedures of collaborative localization for one round are summarized in Algorithm **1**.

6. Simulation

Simulation is first performed to verify the strategies investigated in this study. The motion of revolution half circle is taken, see Figure 7. Here four robots are

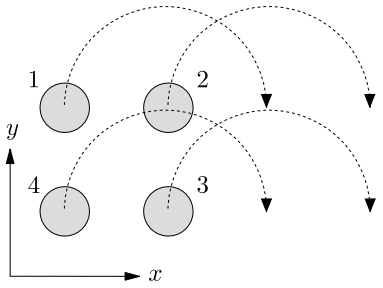

Figure 7. Graphical interpretation of simulated motion: four robots revolution half circle simultaneously

Algorithm 1 Procedures of collaborative localization for one round

all robot members perform distributed EKF based localization and get their respective pose $\hat{\boldsymbol{p}}_i$, $i = 1, 2, \cdots, N$
perform relative observations via infrared distance sensors and gyroscopes, judge and decide relevant pairs of robots, record number of pairs n_p
randomize the index sequence of these n_p pairs of robots
for $h = 1 : n_p$ **do**
  if neither of the two robots in the h-th pair has been corrected by relative observation in this round **then**
    perform correction according to the information from relative observation based on (17)
    record the indices of these two robots in this pair
  end if
end for
feed the further corrected robot poses to position controllers, and go to next round of localization process

simulated with robot size, mass and so on strictly according to the real robots to be used. Each robot keeps a desired distance of 8 cm from its boundary to its neighbors boundaries so as to perform relative observation. Besides these, the robot sensors like odometry, North Star measure functionality, infrared distance sensors and gyroscopes are all mimicked. Very important, the sensor noises are considered so as to demonstrate the simulated robot behavior as close as possible to the real robots.

For verifying our strategies fully, three groups of localization simulation are performed. The first group runs the motion without localization, the second group localizes the robots by EKFs only, while the third group uses EKFs together with robots relative observation. The trajectory of one representative run for each of these three groups are shown in Figure 8.

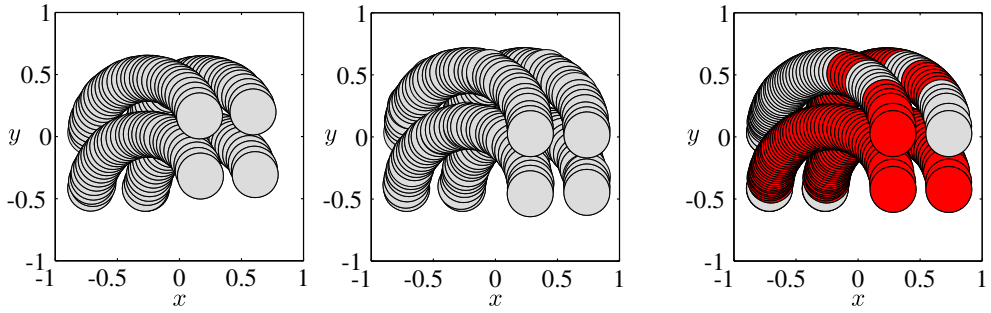

(a) Without localization (b) Based on EKFs (c) Based on EKFs and relative observation

Figure 8. Robot trajectories of one representative run

From Figure 8(a) one can see that the four robots final positions deviate to the positive y direction compared to our desired while in Figure 8(b) the robots deviate to the negative y direction. In Figure 8(c) the robots show better results. Thus, the accuracy for the desired final position is improved from the group without localization to the groups with localization, either the EKF based group or the group based on EKF and relative observation. However, the EKF based group keeps a relatively non smooth trajectory in each specific run although the final position is improved compared to the first group. This is because of the sensor data fusion and the sensor adds noises. Some steps which keep higher prediction

errors contribute to the non smoothnesses of the trajectory. In Figure 8(c) the steps in red color are the ones further corrected by their neighbors based on relative observation after the EKFs. One can see that many steps during the localization process are performed with correction based on the information from neighbors. After relative correction, those steps with higher prediction errors are 'calibrated'. To reveal the differences of localization accuracy from the different groups clearer, the localized center positions of each step of one run are recorded, see the robots center trajectories in Figure 9.

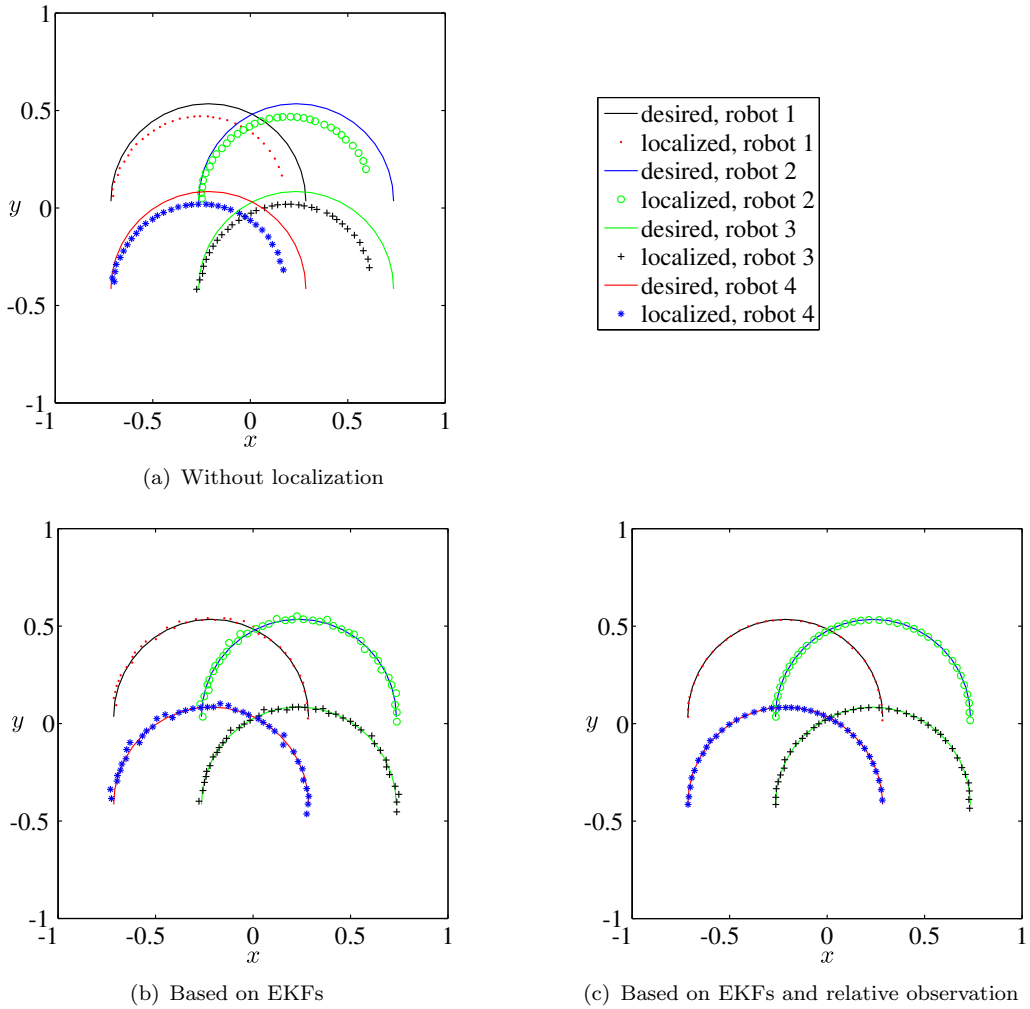

(a) Without localization

(b) Based on EKFs

(c) Based on EKFs and relative observation

Figure 9. Trajectories of robot centers

From Figure 9 one can see that the localization accuracy is clearly improved from no localization to the localization based on EKFs. However, things can be better. In Figure 9(b) the position fluctuation is still too big although the final localized positions are acceptable. The accuracy is further improved by robots relative observation based on multi-source signals, see Figure 9(c). In this case, additional signals are from infrared sensors and gyroscopes. Each group of simulations is performed with 20 runs for making quantitative comparisons. Thus, their average final positions relative to their initial positions, and their position standard deviations correspondingly are listed in Table 1.

After simulation, the investigated strategies are next verified in experiments with real robots.

Table 1. Statistical results of simulation (unit: cm)

	first group	second group	third group
robot 1	$[\bar{x} \;\; \bar{y}] = [87.9 \;\; 11.1]$ $[\sigma_x \;\; \sigma_y] = [0.5 \;\; 2.6]$	$[\bar{x} \;\; \bar{y}] = [99.8 \;\; 0.1]$ $[\sigma_x \;\; \sigma_y] = [0.3 \;\; 1.2]$	$[\bar{x} \;\; \bar{y}] = [99.9 \;\; 0.7]$ $[\sigma_x \;\; \sigma_y] = [0.1 \;\; 0.6]$
robot 2	$[\bar{x} \;\; \bar{y}] = [86.9 \;\; 13.3]$ $[\sigma_x \;\; \sigma_y] = [0.8 \;\; 2.6]$	$[\bar{x} \;\; \bar{y}] = [99.9 \;\; 1.0]$ $[\sigma_x \;\; \sigma_y] = [0.3 \;\; 2.6]$	$[\bar{x} \;\; \bar{y}] = [99.9 \;\; 0.7]$ $[\sigma_x \;\; \sigma_y] = [0 \;\; 0.6]$
robot 3	$[\bar{x} \;\; \bar{y}] = [88.1 \;\; 8.7]$ $[\sigma_x \;\; \sigma_y] = [0.4 \;\; 2.6]$	$[\bar{x} \;\; \bar{y}] = [100.0 \;\; -1.6]$ $[\sigma_x \;\; \sigma_y] = [0.3 \;\; 2.1]$	$[\bar{x} \;\; \bar{y}] = [99.7 \;\; 0.6]$ $[\sigma_x \;\; \sigma_y] = [0.1 \;\; 0.6]$
robot 4	$[\bar{x} \;\; \bar{y}] = [88.4 \;\; 7.6]$ $[\sigma_x \;\; \sigma_y] = [0.3 \;\; 2.6]$	$[\bar{x} \;\; \bar{y}] = [99.5 \;\; -3.0]$ $[\sigma_x \;\; \sigma_y] = [0.3 \;\; 1.5]$	$[\bar{x} \;\; \bar{y}] = [99.7 \;\; 0.6]$ $[\sigma_x \;\; \sigma_y] = [0.1 \;\; 0.6]$

7. Experiments with Real Robots

In order to focus on the relative observation and without losing generality, in the experiments one pair of real robots is investigated and we set up three types of robot motions, see Figure 10.

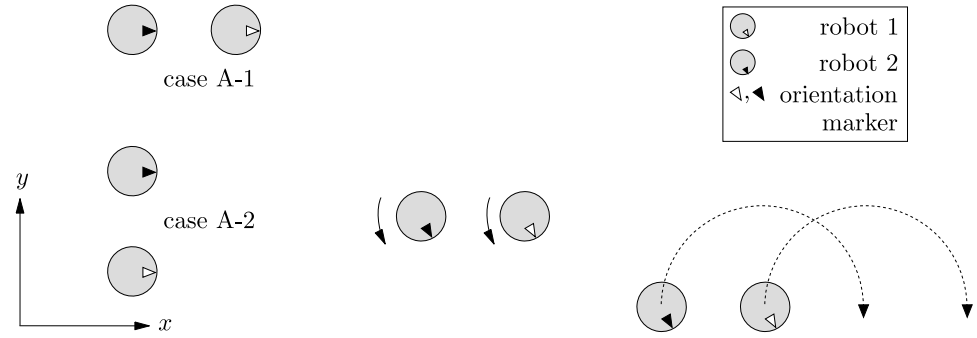

(a) Type A: forward move (b) Type B: spinning (c) Type C: revolution

Figure 10. Three types of motion performed in the experiments with real robots

From Figure 10 one can see that type A is a motion of moving forward in x direction (desired distance 1 meter). It includes the cases of robot 2 following robot 1 (case A-1) and two robots moving in parallel (case A-2). Motion type B is rotating at the original position by 360 degrees (spinning). Finally, type C is a robot revolution along a half circle while keeping the orientation unchanged.

To evaluate the proposed method, three experimental tests (I, II, III) are performed on the mentioned three types of motion (A, B, C). Group I of experiments only uses a single robot and doesn't use EKF estimated pose for position control, i.e., no localization process is considered. Group II also uses a single robot but performs localization based on EKF and the localized pose is used for the closed-loop feedback control. Finally, the third group uses two robots, robot 1 and robot 2 to perform cooperative localization through relative observation based on the results from EKF. Through this we aim to investigate how much of our approach can improve the localization quality. A representative experimental environment is illustrated in Figure 11.

For each motion of each group, this study performs 20 runs. Robot 1 and robot 2 in the two robots cases keep a distance around 8 cm. This is because of the defined relevant regions of robots due to the used infrared distance sensor. According to

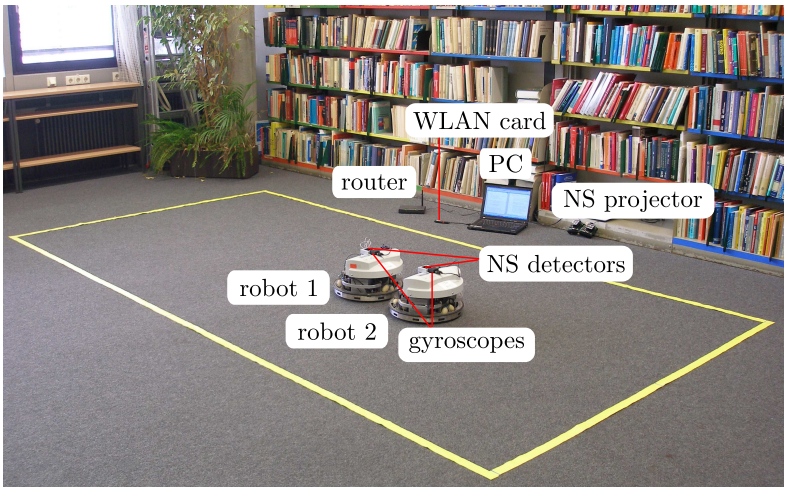

Figure 11. A representative experimental environment for collaborative localization

the modeling in Section 4, for a successful EKF based localization and position control one has to provide the initial process noise covariance $\boldsymbol{Q}(0)$, the initial measurement noise covariance $\boldsymbol{R}(0)$, and the initial estimate error covariance $\boldsymbol{P}(0)$. After many trials and combining the specifications of the used sensors, in EKF based localization and position control experiments the used initial covariances of process and measure noise are $\boldsymbol{Q}(0) = \boldsymbol{diag}(10^{-4},\ 10^{-4},\ (3 \times \pi/180)^2)$ and $\boldsymbol{R}(0) = \boldsymbol{diag}(6.76 \times 10^{-4},\ 6.76 \times 10^{-4},\ (7 \times \pi/180)^2)$, respectively. They all have the units $[\mathrm{m}^2,\ \mathrm{m}^2,\ \mathrm{rad}^2]$. This is so, because we experienced from many tests that the odometry has an accuracy range about $\pm 0.5\,\mathrm{cm}$ for the x and y directions and about $\pm 1.5°$ for the orientation error at the beginning of motion which yields the used initial covariance $\boldsymbol{Q}(0)$ of process noise. This covariance will update since odometry accuracy is changing as long as it moves away from its origin. Similarly, the North Star accuracy range yields our applied measurement noise covariance in which a bigger orientation error is used since the North Star system has a worse measurement for the orientation at the beginning. The initial estimate error covariance is chosen as $\boldsymbol{P}(0) = \boldsymbol{diag}(10^{-4}\,\mathrm{m}^2,\ 10^{-4}\,\mathrm{m}^2,\ (\pi/60)^2\,\mathrm{rad}^2)$ which is equal to $\boldsymbol{Q}(0)$. This is a reasonable choice resulting from the performed tests. The used time step is $\Delta t = 0.01\mathrm{s}$. The update of noise covariance $\boldsymbol{R}(k)$ for each step is according to the North Star noise features while $\boldsymbol{Q}(k)$ is based on the measured data from odometry. During experiments, the basic speed was set to around $200\,\mathrm{mm/s}$.

8. Results and Analysis

In this study, localization is used for robot pose control. After 20 runs for each of the desired motions, their corresponding averaged results are listed in Table 2. The results in this table show the final averaged actual positions or orientations relative to their initial poses, from which one can know that the positioning accuracy is improved by using EKF and further improved by relative observation. However, the orientation error is still too big after EKF sensor data fusion, e.g. in type B in the second group of experiments. The standard deviation also show its oscillating performance, see e.g. in type C of the second group. The oscillating feature was also verified in our simulations in Section 6 for the EKFs based group. This kind of accuracy is significantly improved by relative observation in the third group of experiments, see the results in Table 2.

Taking an example from motion type A, in Table 2 the concerned movement of

forwarding in x direction is recorded and compared. Results show that improvements are significant in which the final position in average is improved from 91.9 cm for the group without localization to 99.9 cm for the group based on EKF. The accuracy is further improved for robot 1 in the third group where one pair of robots have performed relative observation. Correspondingly, the standard deviation σ_x decreases from 5.1 cm to 0.6 cm while in the third group it remains in a small range with average around 0.7 cm.

Table 2. Statistical results of experiments with real robots

type	first group	second group	third group	
A (move 1 meter in x direction, unit: cm)	$\bar{x} = 91.9$ $\sigma_x = 5.1$	$\bar{x} = 99.9$ $\sigma_x = 0.6$	follow	$\bar{x}_1 = 100.0$ $\sigma_{x_1} = 0.8$ $\bar{x}_2 = 99.5$ $\sigma_{x_2} = 1.0$
			parallel	$\bar{x}_1 = 100.1$ $\sigma_{x_1} = 0.5$ $\bar{x}_2 = 100.1$ $\sigma_{x_2} = 0.6$
B (rotate at original, unit: °)	$\bar{\phi} = 325.9$ $\sigma_\phi = 5.1$	$\bar{\phi} = 355.4$ $\sigma_\phi = 1.7$	$\bar{\phi}_1 = 358.9$ $\sigma_{\phi_1} = 1.6$ $\bar{\phi}_2 = 360.6$ $\sigma_{\phi_2} = 1.7$	
C (revolution half circle, unit: cm)	$[\bar{x}\ \bar{y}] =$ [88.0 7.2] $[\sigma_x\ \sigma_y] =$ [3.6 9.1]	$[\bar{x}\ \bar{y}] =$ [99.3 –1.3] $[\sigma_x\ \sigma_y] =$ [0.9 3.7]	$[\bar{x}_1\ \bar{y}_1] = [100.3\ 0.8]$ $[\sigma_{x_1}\ \sigma_{y_1}] = [0.8\ 0.5]$ $[\bar{x}_2\ \bar{y}_2] = [100.0\ 0.8]$ $[\sigma_{x_2}\ \sigma_{y_2}] = [0.8\ 0.5]$	

Compared to robot 1, robot 2 has a slight deterioration in case A-1. In case A-2 the robots move in parallel and reach relatively better results compared to case A-1 where robots move one after the other. The reason is that in case A-2 each robot has more infrared sensors joined for relative observation due to the hardware installation and robots relative position in different cases. Compared to the simulation, the correction from relative observation in the experiments is more effective. The reason is probably because the relative correction on real robots handles more uncertainties which haven't been considered in simulation. Actually, deviations not only happen in the main direction of the motions, e.g., in type A motion robots also have deviations in y direction and orientation. The relative observation based group demonstrates superior performance on this aspect, too. For example, from Table 2 one already knows that a single robot's localization accuracy based on EKF is comparable to the localization performance from the EKF and relative observation mixed group. However, those two robots relative observation cases show better results in y direction and orientation. Next, we choose randomly one of the runs from motion A. In our analysis, it is assumed that position controllers can exactly command the robot to the localized position, thus final deviations are considered to be only due to the localization inaccuracy, rather than due to the position controller. Under this assumption, one can take the localized

poses as robots actual poses.

Figures 12 and 13 show the deviation in y direction and the orientation deviation of a single robot over time, respectively, for motion type A based on EKF localization. The deviation in y direction falls in the range of $[-2\,\text{cm}, 0.4\,\text{cm}]$ while orientation errors are within $[-2.8\,°, 6.4\,°]$. Similarly, for these two dimensions results for the collaborate two robots relative observation cases are also demonstrated, see Figures 14-21.

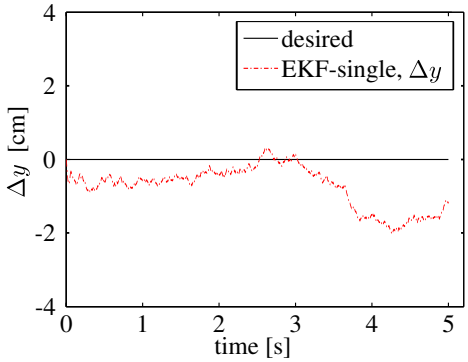

Figure 12. Deviations of y direction of motion type A, single robot localization based on EKF

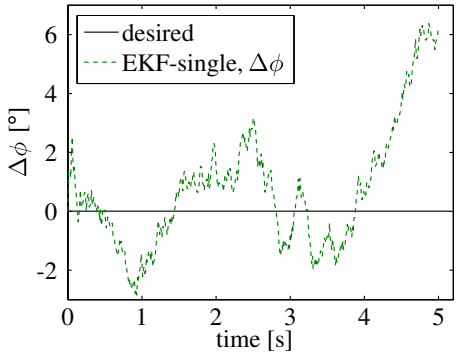

Figure 13. Orientation deviations of motion type A, single robot localization based on EKF

Figures 14-17 present two robots deviations in y direction and orientation of one of 20 runs in case A-1, i.e., one moves after the other. Deviations in y direction of robot 1 are reduced to the range of $[-0.7\,\text{cm}, 0.4\,\text{cm}]$, see Figure 14, while orientation errors almost decrease to only half of the errors from the single robot EKF based localization. The results of robot 2 in case A-1 is slightly inferior to robot 1. However, it is better than those single robot cases, see details in Figures 16 and 17.

For comparisons, this study also extracts the data of two robots moving parallel in x direction based on their own EKF localization and combined with relative observation. As mentioned previously, due to different numbers of sensors joined for relative observations the robots parallel move obtains better localization quality compared to the case of one moves after the other. This is also visible in Figures 18 and 19 in which deviations of robot 1 are shown while performances of robot 2 are revealed in Figures 20 and 21.

Similarly, considerable improvements can also be demonstrated in motion types B and C, see the statistics in Table 2. Results obtained from experiments with real robots show that the proposed methods are feasible and robots collaborative localization based on relative observation reaches a better accuracy. It approximately reduces the variation range to half of the no collaboration cases, and with more data centralization compared to EKF based method. The proposed EKF and relative observation based method can realize multi-robot localization with a promising accuracy. The uncertainties can be effectively reduced compared to the motions without collaboration.

Distinguishing from other researches which also focus on omnidirectional mobile robot localization like (Wu 2005) and (Liu et al. 2008), this study pays more attention to swarm behavior, i.e., cooperative localization of omnidirectional mobile robots in a systematic way. Comparing to (Eberhard and Tang 2013) where the odometry correction is used before using EKF, this study uses measurements from a variety of sensors for improving the localization through EKF and relative observation under a natural mixture scheme.

Traditionally, many schemes also fuse the multiple sensors signals directly. For

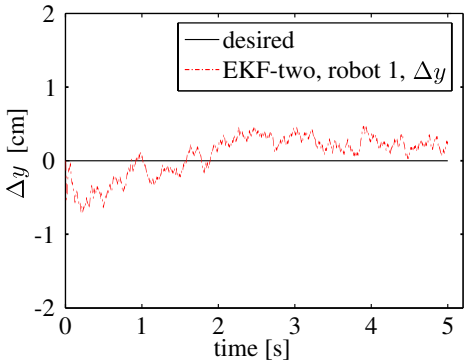

Figure 14. Deviations y direction of robot 1 in case A-1

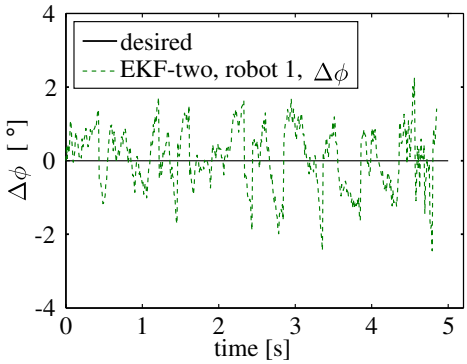

Figure 15. Orientation deviations of robot 1 in case A-1

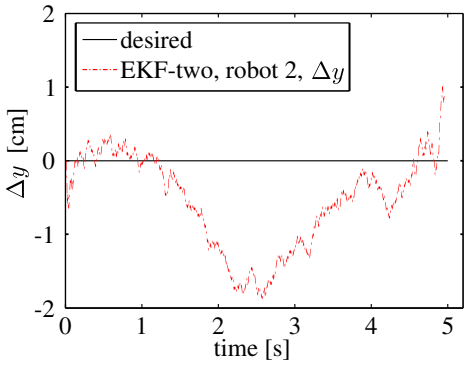

Figure 16. Deviations y direction of robot 2 in case A-1

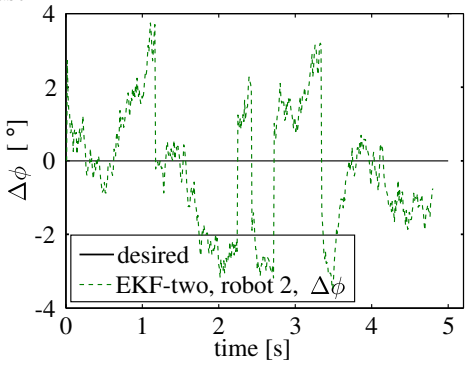

Figure 17. Orientation deviations of robot 2 in case A-1

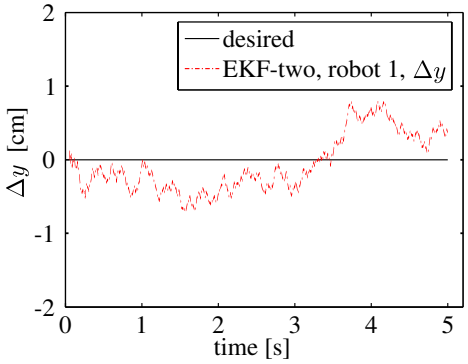

Figure 18. Deviations y direction of robot 1 in case A-2

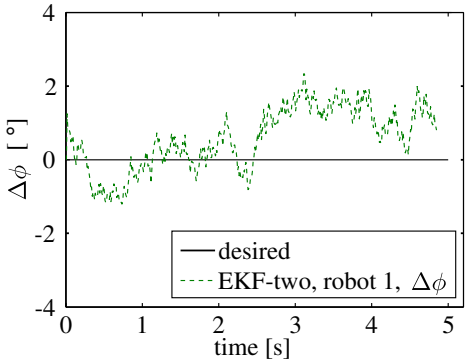

Figure 19. Orientation deviations of robot 1 in case A-2

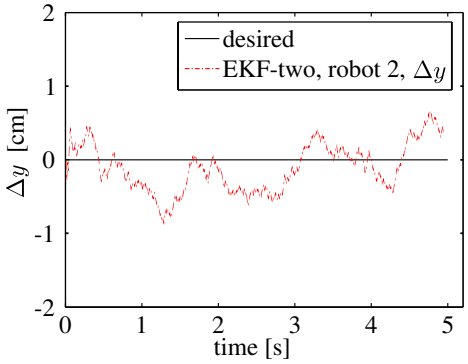

Figure 20. Deviations y direction of robot 2 in case A-2

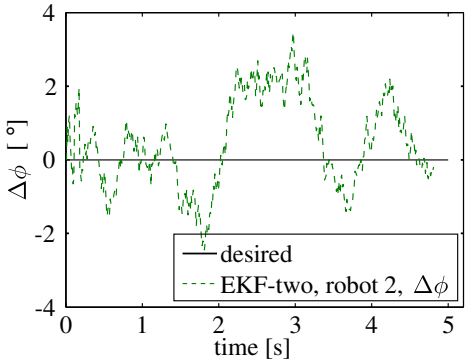

Figure 21. Orientation deviations of robot 2 in case A-2

example, in this application researchers also can directly fuse data from odometry, North Star and gyroscope. We have tested this scheme in our experiments, too. However, the results are not so appreciated, particularly for long-term running. The reason is quite clear for us. Relative observation in our case is mainly used to improve the localization belief (certainty), rather than to improve the accuracy of localization itself. If gyroscope joins the data fusion directly, it won't contribute to the improvement of localization beliefs (certainties) of x and y positions. It actually only improves the orientation estimation. Whereas, by using our proposed 'uncertainty volume' strategy and letting the gyroscope for external relative measurement, the further corrections of position and orientation are coupled and positively mutual affected, i.e., it increases the localization certainty for both translational x and y positions, and orientation as well. This improvement becomes more significant when the robots perform a long-term running. Besides this, our study wants to keep the advantage of less computational cost. The situation of more sensors directly join for the data fusion will inevitably increase the calculation burden which is not pursued by us. Otherwise, many mature solutions introduced in Section 2 will be already the good choices.

9. Conclusions

This paper investigates the robot localization issue, particularly oriented to multi-robot collaborative localization. For this purpose a method based on EKF for a single robot is developed, and then a distributed EKF and relative observation combined approach has been outlined. For updating the robots beliefs during relative observation, the idea of an 'uncertainty volume' is provided. Both the simulation and experimental results from no localization, pure EKF localization and EKF-relative observation based cooperative localization are compared. This confirmed the feasibility of an EKF-relative observation mixed methodology. From the comparison, one can see that the proposed technique shows promising results when compared with those only based on EKFs without collaboration. The reduction of computational complexity is also considered where a conservative update scheme for the prediction covariance is used. This is highly beneficial in real world applications where robots need to actually perform tasks rather than just to localize precisely. The implementation details like process and measurement noises show their reference value, too. Through the distributed EKF and relative observation this study constitutes a means for fusing measurements collected from a variety of sensors with lower burden of communication and processing requirements. It gives a contribution in the direction of robot localization which is one of the main requirements for mobile robots. It is the hope of this study that such an EKF-relative observation mixed investigation can be taken as a new realization for multi-robot collaborative localization.

References

Bliesener, M., Weber, C., Kling, K., Karras, U., and Zitzmann, D. (2007), *Festo Robotino Manual*, Festo Didactic GmbH & Co. KG, Denkendorf, Germany.

Caglioti, V., Citterio, A., and Fossati, A. (2006), 'Cooperative, Distributed Localization in Multi-robot Systems: a Minimum-entropy Approach,' in *IEEE Workshop on Distributed Intelligent Systems: Collective Intelligence and Its Applications*, June 15–16, Prague, Czech Republic, pp. 25–30.

Cao, M.M. (2009), 'Dynamic Behavior Path Planning of Mobile Robot Based on Fuzzy Logic Control (in Chinese),' Master Thesis, Beijing Jiaotong University.

Dhariwal, A., and Sukhatme, G. (2007), 'Experiments in Robotic Boat Localization,' in *Proceedings of the IEEE/RSJ International Conference on Intelligent Robots and Systems*, October 29–November 2, San Diego, USA, pp. 1702–1708.

Eberhard, P., and Tang, Q. (2013), 'Sensor Data Fusion for the Localization and Position Control of One Kind of Omnidirectional Mobile Robots,' in *Multibody System Dynamics, Robotics and Control*, eds. J. Gerstmayr and H. Gattringer, Wien: Springer, pp. 45–74.

Elor, Y., and Bruckstein, A.M. (2012), 'A "Thermodynamic" Approach to Multi-robot Cooperative Localization,' *Theoretical Computer Science*, 457, 59–75.

Ferdaus, S.N. (2008), 'A Topological Approach to Online Autonomous Map Building for Mobile Robot Navigation,' Master Thesis, Memorial University of Newfoundland.

Fox, D., Burgard, W., Kruppa, H., and Thrun, S. (2000), 'A Probabilistic Approach to Collaborative Multi-robot Localization,' *Autonomous Robots*, 8, 325–344.

Franklin, S.J., Finn, A., Pattison, J.E., and Jain, L.C. (2010), 'Motion Optimization Scheme for Cooperative Mobile Robots,' (Vol. 304), eds. A. Finn and L.C. Jain, Berlin: Springer, pp. 139–173.

Gasparri, A., Panzieri, S., and Pascucci, F. (2009), 'A Spatially Structured Genetic Algorithm for Multi-robot Localization,' *Intelligent Service Robotics*, 2, 31–40.

Grabowski, R., Navarro-Serment, L.E., Paredis, C., and Khosla, P. (2000), 'Heterogeneous Teams of Modular Robots for Mapping and Exploration,' *Autonomous Robots*, 8, 293–308.

Grewal, M.S., and Andrews, A.P. (2008), *Kalman Filtering: Theory and Practice Using MATLAB* (3 ed.), Hoboken: John Wiley & Sons.

Howard, A., Matark, M.J., and Sukhatme, G.S. (2002), 'Localization for Mobile Robot Teams Using Maximum Likelihood Estimation,' in *IEEE/RSJ International Conference on Intelligent Robots and Systems* (Vol. 1), September 30–October 4, Lausanne, Switzerland, pp. 434–439.

Kalman, R.E. (1960), 'A New Approach to Linear Filtering and Prediction Problems,' *Basic Engineering*, 82, 35–45.

Lee, K., Doh, N.L., Chung, W.K., Lee, S.K., and Nam, S.Y. (2008), 'A Robust Localization Algorithm in Topological Maps with Dynamic Noises,' *Industrial Robot: An International Journal*, 35, 435–448.

Liu, Y., Zhu, J.J., Williams, R.L., and Wu, J. (2008), 'Omni-directional Mobile Robot Controller Based on Trajectory Linearization,' *Robotics and Autonomous Systems*, 56, 461–479.

Maaref, H., and Barret, C. (2002), 'Sensor-Based Navigation of a Mobile Robot in an Indoor Environment,' *Robotics and Autonomous Systems*, 38, 1–18.

Madhavan, R., Fregene, K., and Parker, L. (2004), 'Distributed Cooperative Outdoor Multirobot Localization and Mapping,' *Autonomous Robots*, 17, 23–39.

Marchetti, L., Grisetti, G., and Iocchi, L. (2007), 'A Comparative Analysis of Particle Filter Based Localization Methods,' in *RoboCup 2006: Robot Soccer World Cup X, Lecture Notes in Computer Science* (Vol. 4434), eds. G. Lakemeyer, E. Sklar, D.G. Sorrenti and T. Takahashi, Berlin: Springer, pp. 442–449.

McLurkin, J. (2009), 'Measuring the Accuracy of Distributed Algorithms on Multi-robot Systems with Dynamic Network Topologies,' in *Distributed Autonomous Robotic Systems 8*, eds. H. Asama, H. Kurokawa, J. Ota and K. Sekiyama, Berlin: Springer, pp. 15–26.

Molhim, M. (2002), 'Fuzzy Logic Based Localization for Mobile Robots,' Doctoral Thesis, Concordia University.

Murillo, A.C., Guerrero, J.J., and Sagüés, C. (2007), 'Topological and Metric Robot Localization through Computer Vision Techniques,' in *IEEE Workshop From Features to Actions: Unifying Perspectives in Computational and Robot Vision Held with IEEE International Conference on Robotics and Automation*, April 10–14, Rome, Italy, pp. 79–85.

Özkucur, N.E., Kurt, B., and Akın, H.L. (2009), 'A Collaborative Multi-robot Localization Method without Robot Identification,' in *RoboCup 2008: Robot Soccer World Cup XII, Lecture Notes in Computer Science* (Vol. 5399), eds. L. Iocchi, H. Matsubara,

A. Weitzenfeld and C. Zhou, Berlin: Springer, pp. 189–199.

Roumeliotis, S.I., and Bekey, G.A. (2002), 'Distributed Multirobot Localization,' *IEEE Transactions on Robotics and Automation*, 18, 781–795.

Tang, Q., and Eberhard, P. (2011), 'A PSO-based Algorithm Designed for a Swarm of Mobile Robots,' *Structural and Multidisciplinary Optimization*, 44, 483–498.

Tang, Q. (2012), 'Cooperative Search by Mixed Simulated and Real Robots in a Swarm Based on Mechanical Particle Swarm Optimization,' Doctoral Thesis, Institute of Engineering and Computational Mechanics, University of Stuttgart, No. 25. Aachen: Shaker Verlag.

Thrun, S., Burgard, W., and Fox, D. (2005), *Probabilistic Robotics*, Cambridge: MIT Press.

Thrun, S. (1998), 'Bayesian Landmark Learning for Mobile Robot Localization,' *Machine Learning*, 33, 41–76.

Wang, L., Cai, X., Fan, W., and Zhang, H. (2009), 'An Improved Method for Multi-Robot Cooperative Localization Based on Relative Bearing,' in *Proceedings of the IEEE International Conference on Robotics and Biomimetics*, February 21-26, Bangkok, Thailand, pp. 1862–1867.

Wu, J.H. (2005), 'Dynamic Path Planning of an Omni-directional Robot in a Dynamic Environment,' Doctoral Thesis, Ohio University.

Yang, Y. (2008), 'Probabilistic Path Planning with Extended Local Planners,' Doctoral Thesis, Purdue University.